ChemComm

COMMUNICATION

View Article Online
View Journal | View Issue

Cite this: *Chem. Commun.*, 2026, **62**, 534

Received 1st November 2025,
Accepted 26th November 2025

DOI: 10.1039/d5cc06233k

rsc.li/chemcomm

Nickel-catalyzed dehydrogenative Zn–Zn coupling to a Zn(I) dimer and its reactivity

Sagrika Rajput, Smrutirani Padhan, Nithya M. Thilakan, Sayantan Mukhopadhyay and Sharanappa Nembenna *

High-yield access to a bis-guanidinate zinc(I) dimer was achieved *via* nickel-catalyzed dehydrocoupling of a zinc(II) hydride. Reactions of Zn(I) dimer with diphenyl dichalcogenides and sulfur resulted in the formation of zinc chalcogenolates and a rare zinc(II) hexasulfide, respectively. Protonolysis of the zinc chalcogenolates afforded zinc hydroxide or phenoxide complexes.

N,*N*′,*N*″,*N*‴-Tetra-substituted guanidinate anions are widely used to stabilize metal complexes across the periodic table.[1] In contrast, their bis-guanidinate (NacNac analogue) counterparts remain largely unexplored,[2] despite the long-known chemistry of biguanides.[3] Moreover, the chemistry of bis-guanidinate (BG) zinc species, including Zn(I) and Zn(II) hydrides, is scarcely explored.[4] A landmark in Zn(I) chemistry was Carmona's synthesis of the pentamethylcyclopentadienyl zinc(I) dimer [Cp*ZnZnCp*], which established the foundation for Zn–Zn bond chemistry.[5] Subsequently, this field expanded, with such low oxidation state zinc(I) dimers being accessed *via* ligand substitution reactions of Carmona's zinc(I) complex or by reductive coupling of ligated zinc(II) halides with stoichiometric metal reagents.[6] Metal-catalyzed dehydrocoupling provides an efficient route to E–E bond formation in p-block systems (groups 13–15), forming B–B, Si–Si, and P–P bonds.[7] Regarding metal-catalyzed Zn–Zn bonded complexes, the Xu group reported the first catalytic method for Zn–Zn bond formation *via* Ni(0)-catalyzed dehydrocoupling of Zn(II) hydrides.[8] Recently, Crimmin and coworkers reported the Ni(I)-catalyzed dehydrocoupling of zinc hydride using $[Ni(CO)Cp]_2$ as a catalyst, affording the known NacNac Zn(I) dimer.[9] Such protocols offer several advantages, including atom economy, avoidance of hazardous metal reagents, and the generation of only hydrogen gas as a byproduct. However, the above protocols are limited to β-diketiminate (NacNac) stabilized zinc(I) dimers. Further, low-oxidation state Zn(I) complexes are remarkably stable,[6a,10] often retaining the Zn–Zn bond upon reaction with Lewis bases or protic substrates.[10b,11] Zn(I) species have been used to stabilize transition metals,[12] exhibit interesting electrochemical behaviour,[13] and display catalytic activity in hydroamination[14] and hydroboration.[4d] However, selective Zn–Zn bond activation or insertion remains uncommon.[6b,c,15] Notably, in 2025, the Crimmin group reported group 13 carbene analogue insertion into a Zn–Zn bond.[16] Schulz group demonstrated the reaction of a β-diketiminate-supported Zn–Zn complex with diphenyl dichalcogenides (Ph_2E_2; E = Se, Te), forming LZnEPh complexes.[17] In 2023, Xu and co-workers described the reaction of an NNP ligand(L′)-supported Zn–Zn bonded complex with Ph_2S_2 to form Zn(II) thiolate.[18] Overall, the chemistry of dichalcogenide insertion into Zn–Zn bonds remains at an early stage. Furthermore, despite significant advances in molecular zinc hydride chemistry,[19] the dehydrocoupling of zinc hydrides with arylchalcogenol or diphenyl dichalcogenides to form zinc chalcogenolates remains rare.[19d] Thus, herein, we report the synthesis of the known bis-guanidinate zinc(I) complex *via* Ni(0)-catalyzed dehydrocoupling of zinc hydride. Further, we report a series of well-defined bis-guanidinate (BG)-stabilized zinc chalcogenolate complexes. More importantly, we report the first example of a rare neutral *N*,*N*′-chelated bis-guanidine zinc hexasulfide complex. Dehydrocoupling of $\mathbf{[L^1ZnH]_2}$ was carried out using $Ni(CO)_2(PPh_3)_2$ as a catalyst to afford the bis-guanidinate-supported Zn–Zn bonded complex $\mathbf{(L^1ZnZnL^1)}$ (where L^1 = {(ArHN)(ArN)C═N–C(NAr)(NHAr)}, Ar = 2,6-$Et_2C_6H_3$) in good yield (87%) (Scheme 1). In contrast, dehydrocoupling of $\mathbf{L^2ZnH}$ (L^2 = {(ArHN)(ArN)C═N–C(NAr)(NHAr)}, Ar = 2,6-$^i Pr_2C_6H_3$)

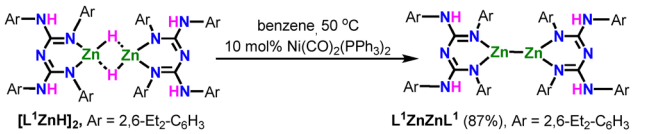

Scheme 1 Nickel-catalyzed synthesis of bis-guanidinate Zn(I) dimer.

School of Chemical Sciences, National Institute of Science Education and Research (NISER), Homi Bhabha National Institute (HBNI), Bhubaneswar, 752050, India. E-mail: snembenna@niser.ac.in

under forcing conditions (15 mol% Ni Cat., 80 °C, 48 h) did not produce the Zn(I) dimer, indicating steric hindrance from the *N*-aryl substituents of BG.

Notably, **[L¹ZnH]₂** showed no dehydrocoupling in the absence of a Ni catalyst at 80 °C, also confirming the essential role of the Ni catalyst. The formation of **L¹ZnZnL¹** was monitored by *in situ* ^{1}H NMR spectroscopy during the Ni-catalyzed dehydrocoupling of **[L¹ZnH]₂** from room temperature to 50 °C. At rt, no change was observed; however, heating to 50 °C led to the gradual disappearance of the Zn–*H* signal (4.5 ppm). After 4 h at 50 °C, a new signal at 4.81 ppm corresponding to Ar–N*H* of **L¹ZnZnL¹** began to appear, and after 30 h, complete formation of **L¹ZnZnL¹** was achieved (see SI). To gain further mechanistic insight, a stoichiometric reaction between **[L¹ZnH]₂** and $Ni(CO)_2(PPh_3)_2$ was carried out (Scheme 2). The reaction yielded a hydride-bridged Zn–Ni heterobimetallic complex **[Zn–Ni]#**, as confirmed by multinuclear NMR spectroscopy. In the ^{1}H NMR spectrum, the Ar–N*H* resonance of the bis-guanidinate ligand of **[Zn–Ni]#** appears at 5.09 ppm, while a distinct signal as a doublet at −3.60 to −3.66 ppm corresponds to the bridging hydride, unambiguously confirming the formation of the Zn–Ni heterobimetallic species.[8] ^{1}H NMR monitoring revealed approximately 50% conversion to the heterobimetallic complex after 12 h at rt, with no further change thereafter, indicating the establishment of an equilibrium. Upon heating the reaction mixture to 50 °C, **[L¹ZnH]₂** reacted with **[Zn–Ni]#**, shifting the equilibrium toward the formation of **L¹ZnZnL¹**. To evaluate the possibility of a radical pathway, **[L¹ZnH]₂** was treated with 10 mol% $Ni(CO)_2(PPh_3)_2$ in the presence of TEMPO, which showed no inhibition or change in product formation, thereby excluding the participation of radical intermediates. Kinetic studies of the catalytic dehydrocoupling reaction were conducted by varying the catalyst loading (10–20 mol%) and monitoring the reaction progress *via* ^{1}H NMR spectroscopy. The reactions exhibited zero-order kinetics with respect to the zinc hydride concentration, while a first-order dependence on the Ni-catalyst concentration was observed (Fig. S8–S12, SI). Based on these findings, a plausible mechanism for the Ni-catalyzed Zn–Zn bond formation is proposed (Scheme 3). The catalytic cycle is initiated by coordination of the Zn–H bond to the Ni center, forming a heterobimetallic complex **[Zn–Ni]#**. Further, reaction of **[Zn–Ni]#** with another equivalent of zinc hydride to generate a hydride-bridged species (**Int-1**). Owing to its inherent instability, **Int-1** further reacts with an additional molecule of zinc hydride to afford **L¹ZnZnL¹**, with concomitant H_2 elimination. Regeneration of the heterobimetallic complex closes the catalytic cycle. Further, bis-guanidinate (BG)-stabilized zinc chalcogenolate complexes (**Zn-1**, **Zn-2**, and **Zn-3**) were synthesized *via* reaction of the **L¹ZnZnL¹** with Ph_2E_2 (E = S, Se, or Te), yielding (L^1ZnEPh)

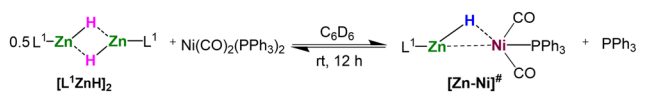

Scheme 2 Stoichiometric reaction.

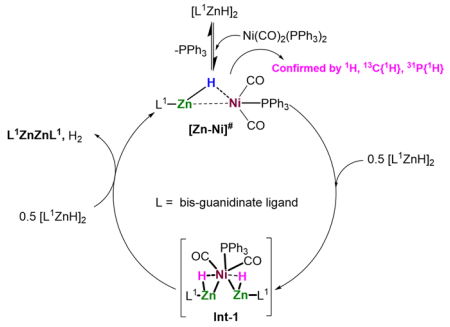

Scheme 3 Proposed catalytic cycle for the formation of bis-guanidinate Zn(I) dimer.

species (Scheme 4). In addition, we developed a route wherein dimeric **[L¹ZnH]₂** undergoes dehydrocoupling with Ph_2E_2 to yield the same class of zinc chalcogenolates (**Zn-1** to **Zn-3**, Scheme S4, SI). Likewise, bulky **L²ZnH** treated with 0.5 equivalents of Ph_2E_2 to produce L^2ZnEPh complexes (**Zn-4**, **Zn-5**, and **Zn-6**; Scheme S5, SI). All zinc chalcogenolates (**Zn-1** to **Zn-6**) were thoroughly characterized by multinuclear NMR, high-resolution mass spectrometry (HRMS), and single-crystal X-ray diffraction. Complexes **Zn-1–Zn-6** are moderately sensitive to air and moisture. The ^{1}H NMR spectra (C_6D_6) of complexes **Zn-1–Zn-3** show downfield-shifted Ar–N*H* signals at 5.04–5.06 ppm compared to 4.81 ppm for **L¹ZnZnL¹** (Scheme 4). The Zn–H resonance at 4.5 ppm disappears (Scheme S4 and Method B, SI), confirming Zn–*H* consumption during complexation. Similarly, **Zn-4–Zn-6** exhibit disappearance of the Zn–*H* signal at 4.42 ppm (**L²ZnH**) and new Ar–N*H* resonances at 5.78–5.85 ppm. The $^{13}C\{^1H\}$ NMR spectra of **Zn-1–Zn-6** display characteristic N_3C signals between 157.1–157.6 ppm, consistent with the formation of zinc bis-guanidinate complexes.[4] Incorporation of selenium (Se) and tellurium (Te) was unequivocally confirmed by ^{77}Se and ^{125}Te NMR spectroscopy. **Zn-2** and **Zn-5** showed ^{77}Se singlets at −26 and −19 ppm, respectively, while **Zn-3** and **Zn-6** exhibited ^{125}Te resonances at −273 and −264.5 ppm, respectively.[20] Crystallographic details of compounds **Zn-1–Zn-6** are summarized in Tables S1 and S2 (SI). Solid-state structures revealed that zinc chalcogenolates **Zn-1** and **Zn-2** adopt dimeric structures, whereas **Zn-3** to **Zn-6** are monomeric (Fig. 1). The Zn–S bond lengths are 2.3514(8) Å in **Zn-1** and 2.2147(15) Å in **Zn-4**. Compared to Xu's L′ZnSPh complex [2.2645(4) Å],[18] the Zn–S bond in **Zn-1** is longer, whereas that in **Zn-4** is shorter. The N1–Zn1–N2 bite angles are 94.65(10)° and 96.93(17)° in **Zn-1** and **Zn-4**, respectively, both of which are acute than that reported for L'ZnSPh [98.54(4)°].[18] The Zn–Se bond distances in **Zn-2** [2.4595(7)–2.5317(8)] Å are

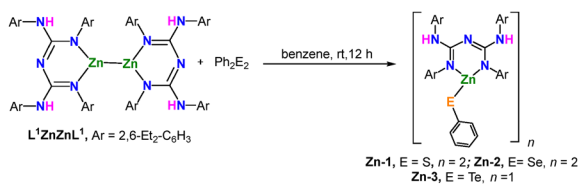

Scheme 4 Synthesis of **Zn-1**, **Zn-2**, and **Zn-3** complexes.

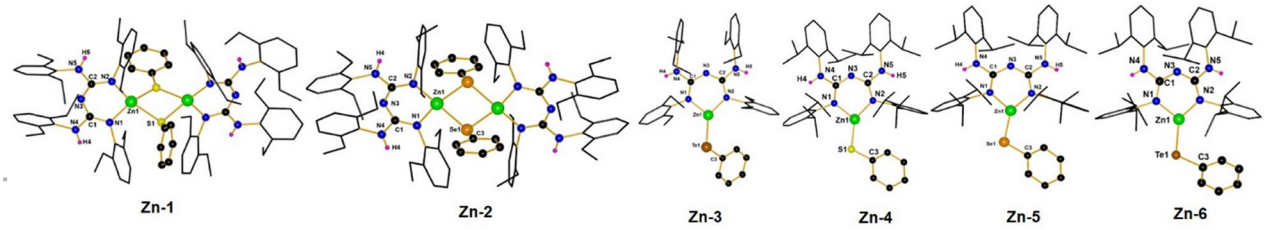

Fig. 1 Molecular structures of **Zn-1** to **Zn-6**.

comparable to those reported for [(^{Mes}NacNac)ZnSePh]$_2$ [2.4291(5)–2.5951(6) Å],[17] whereas **Zn-5** [2.3058(7)] Å exhibits a slightly shorter Zn–Se bond. The N1–Zn1–N2 bite angles are 97.19(15)° in **Zn-2** and 97.0(15)° in **Zn-5**, which are comparable to the reported [^{Mes}NacNacZnSePh]$_2$ complex [97.66(6)°].[17] Zn–Te bond distances in **Zn-3** (2.5023(5) Å) and **Zn-6** (2.5031(8) Å) are slightly shorter than reported in [Zn(TePh)$_2$][TMEDA]^{21}-(2.5769(14) Å). The N–Zn–N bite angles are 96.59(14)° for **Zn-3** and 97.73(11)° for **Zn-6**, slightly acute than that in [Zn(TePh)$_2$]-[TMEDA] (98.1(4)°).[21]

Given our interest in the synthesis and reactivity studies of bis-guanidinate zinc(I) dimers, and considering the scarcity of studies on Zn–Zn reactivity with sulfur (see Scheme S6, SI).[15h,18] We set out to investigate the reactivity of the zinc(I) dimer with elemental sulfur (S_8). It is important to note that the activation of S_8 by a Zn–Zn bonded species to form zinc polysulfide complexes has not yet been reported. Such zinc polysulfides have significant importance in the fields of materials and bioinorganic chemistry.[22] Remarkably, the reaction between **L^{1}ZnZnL^1** and S_8 in benzene afforded a zinc hexasulfide complex (**Zn-7**), in which the bis-guanidinate ligand transformed from a monoanionic (LX-type) to a neutral donor (L_2-type) (Scheme 5). This ligand transformation was presumably due to zinc-mediated H atom abstraction from the solvent. In contrast, no reaction occurred between **[L^{1}ZnH]$_2$** and S_8 under identical conditions, highlighting the crucial role of the Zn(I) species in sulfur activation. **Zn-7** featured a zinc center in a distorted tetrahedral geometry within a six-membered N_3C_2Zn and seven-membered ZnS_6 metallacycles, representing a rare,[22a,22b] structurally characterized bis-guanidine zinc(II)–polysulfide complex.

The ^{1}H NMR spectrum exhibited the characteristic bis-guanidinate N*H* resonances, featuring a singlet at 4.95 ppm (1H) attributed to the central backbone N–*H* proton (N_3H) and a singlet at 5.07 ppm (2H) corresponding to the Ar–N*H* backbone protons (N_4H and N_5H; Fig. 2). Zn–S bond distances ranged from 2.2681(8) to 2.3180(9) Å, which are comparable to

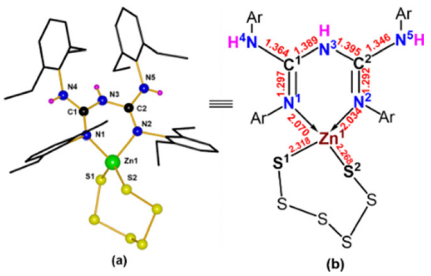

Fig. 2 (a) Molecular structure of **Zn-7**. (b) ChemDraw diagram with bond parameters.

previously reported Schulz's [^{Mes}NacNacS]$_2$Zn compound, (2.273(7)–2.279(8) Å)[15h] (Fig. 2).

Furthermore, the reactions of **Zn-1** with degassed H_2O and **Zn-2** with phenol (PhOH) afforded the corresponding zinc hydroxide (**Zn-8**) and zinc phenoxide complexes (**Zn-9**), respectively (Scheme 6). Soluble molecular zinc hydroxides are rare,[23] and this work presents the first example of a structurally characterized bis-guanidinate-stabilized zinc hydroxide complex. Compounds **Zn-8** and **Zn-9** were thoroughly characterized by standard spectroscopic methods, including single-crystal X-ray diffraction. The ^{1}H NMR spectrum of **Zn-8** in C_6D_6 showed a singlet at δ −0.01 ppm corresponding to the –O*H* proton of a Zn–μ–OH–Zn bridge, comparable with the μ–OH resonance reported for [^{Mes}NacNacZnOH]$_2$ at δ −0.20 ppm, while the remaining signals were well in agreement with the bis-guanidinate ligand framework.[2] The presence of a Zn–OH bond was further corroborated by a broad IR absorption band at 3703 cm^{-1}, which is characteristic of Zn–OH stretching vibrations.[23] In compound **Zn-9**, the ^{1}H NMR spectrum displayed the Ar–N*H* backbone resonance at 4.96 ppm, consistent with the formation of a bis-guanidinate phenoxide complex.[4e] Crystallographic details of compounds **Zn-8**–**Zn-9** are summarized in Table S3 (SI). The Zn–O bond lengths in **Zn-8** [1.9638(19)–2.0036(19) Å] are

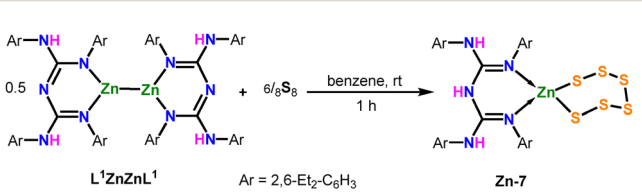

Scheme 5 Synthesis of bis-guanidine zinc(II) hexasulfide complex.

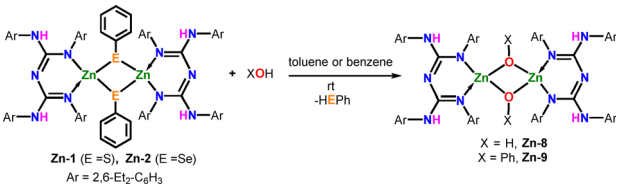

Scheme 6 Synthesis of bis-guanidinate-supported zinc complexes (**Zn-8**, **Zn-9**).

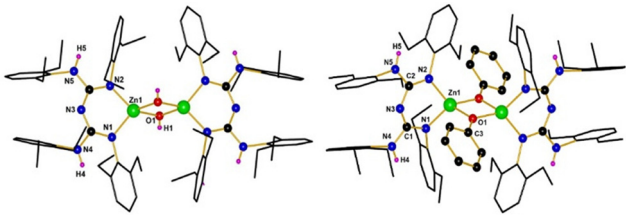

Fig. 3 Molecular structures of **Zn-8** (left) and **Zn-9** (right).

comparable to those reported for a ^{Mes}NacNac-supported zinc hydroxide complex [1.9623(10)–1.9890(11) Å].[23c] In compound **Zn-9**, the Zn–O bond distances [1.9682(19)–2.0449(19) Å] are comparable to the range observed for a bis-guanidinate zinc alkoxide complex [1.972(2)–2.040(2) Å].[4e] The N–Zn–N bite angle in **Zn-8** is 94.62(9)°, which is slightly acute than that observed for [^{Mes}NacNac–ZnOH]$_2$ [98.50(5)°],[23c] while the N–Zn–N bite angle in **Zn-9** [95.05(9)°] is comparable to that reported for a bis-guanidinate zinc alkoxide complex [94.84(10)°][4e] (Fig. 3).

In summary, we report the facile and high-yield synthesis of a known bis-guanidinate zinc(I) dimer *via* dehydrocoupling of the corresponding zinc hydride in the presence of a nickel catalyst. Based on stoichiometric experiments and *in situ* NMR studies, a plausible catalytic cycle for Zn–Zn bond formation was proposed. Furthermore, a series of well-defined bis-guanidinate zinc chalcogenolates was obtained by reacting either the zinc(I) dimer or the bis-guanidinate zinc(II) hydrides with diphenyl dichalcogenides (Ph_2E_2; E = S, Se, Te). Notably, the reaction of the zinc(I) dimer with elemental sulfur produced an unusual neutral bis-guanidine-stabilized zinc(II) hexasulfide. To the best of our knowledge, this represents a rare example of such a species, accessible *via* zinc(I) dimer. Additionally, the reaction of zinc chalcogenolates with H_2O or PhOH affords bis-guanidinate zinc hydroxide or phenoxide complexes. Further reactivity studies of newly synthesized zinc complexes are underway in our lab.

This research was supported by the Science and Engineering Research Board (SERB), India (CRG/2021/007000) and the National Institute of Science Education and Research (NISER), Bhubaneswar, Odisha, Homi Bhabha National Institute (HBNI), Mumbai, Department of Atomic Energy (DAE), Govt. of India.

Conflicts of interest

The authors declare no conflict of interest.

Data availability

The data supporting this article have been included as part of the supplementary information (SI). Supplementary information: ^{1}H, ^{13}C{^{1}H}, ^{31}P{^{1}H}, ^{77}Se, ^{125}Te NMR spectra of compounds. See DOI: https://doi.org/10.1039/d5cc06233k.

CCDC 2482300–2482306, 2496490 and 2496491 contain the supplementary crystallographic data for this paper.[24a–i]

Notes and references

1 (*a*) M. P. Coles, *Dalton Trans.*, 2006, 985–1001; (*b*) F. T. Edelmann, *Chem. Soc. Rev.*, 2009, **38**, 2253–2268; (*c*) A. A. Trifonov, *Coord. Chem. Rev.*, 2010, **254**, 1327–1347; (*d*) F. Carrillo-Hermosilla, R. Fernández-Galán, A. Ramos and D. Elorriaga, *Molecules*, 2022, **27**, 5962; (*e*) C. Jones, *Coord. Chem. Rev.*, 2010, **254**, 1273–1289.
2 T. Peddarao, A. Baishya, N. Sarkar, R. Acharya and S. Nembenna, *Eur. J. Inorg. Chem.*, 2021, 2034–2046.
3 P. Ray, *Chem. Rev.*, 1961, **61**, 313–359.
4 (*a*) R. K. Sahoo, M. Mahato, A. Jana and S. Nembenna, *J. Org. Chem.*, 2020, **85**, 11200–11210; (*b*) R. K. Sahoo, N. Sarkar and S. Nembenna, *Angew. Chem., Int. Ed.*, 2021, **60**, 11991–12000; (*c*) S. Rajput, R. K. Sahoo, N. M. Thilakan and S. Nembenna, *Chem. Commun.*, 2024, **60**, 11148–11151; (*d*) R. K. Sahoo, S. Rajput, A. G. Patro and S. Nembenna, *Dalton Trans.*, 2022, **51**, 16009–16016; (*e*) A. G. Patro, R. K. Sahoo and S. Nembenna, *Dalton Trans.*, 2024, **53**, 3621–3628.
5 I. Resa, E. Carmona, E. Gutierrez-Puebla and A. Monge, *Science*, 2004, **305**, 1136–1138.
6 (*a*) T. Li, S. Schulz and P. W. Roesky, *Chem. Soc. Rev.*, 2012, **41**, 3759–3771; (*b*) A. Stasch, *Chem. – Eur. J.*, 2012, **18**, 15105–15112; (*c*) S. Jiang, S. Xu and X. Xu, *Chem. Commun.*, 2025, **61**, 12085–12096.
7 (*a*) E. C. Neeve, S. J. Geier, I. A. I. Mkhalid, S. A. Westcott and T. B. Marder, *Chem. Rev.*, 2016, **116**, 9091–9161; (*b*) Y. Corey, *Adv. Organomet. Chem.*, 2004, **51**, 1–52; (*c*) R. J. Less, R. L. Melen, V. Naseri and D. S. Wright, *Chem. Commun.*, 2009, 4929–4937.
8 S. Jiang, Y. Cai, A. Carpentier, I. Del Rosal, L. Maron and X. Xu, *Chem. Commun.*, 2021, **57**, 13696–13699.
9 M. Perez-Jimenez, B. L. Geoghegan, A. Collauto, M. M. Robetaler and M. R. Crimmin, *Angew. Chem., Int. Ed.*, 2024, **63**, e202411828.
10 (*a*) A. Grirrane, I. Resa, A. Rodríguez and E. Carmona, *Coord. Chem. Rev.*, 2008, **252**, 1532–1539; (*b*) S. Gondzik, D. Bläser, C. Wölper and S. Schulz, *Chem. – Eur. J.*, 2010, **16**, 13599–13602; (*c*) E. Carmona and A. Galindo, *Angew. Chem., Int. Ed.*, 2008, **47**, 6526–6536.
11 (*a*) D. Schuchmann, U. Westphal, S. Schulz, U. Flörke, D. Bläser and R. Boese, *Angew. Chem., Int. Ed.*, 2009, **48**, 807–810; (*b*) S. Schulz, S. Gondzik, D. Schuchmann, U. Westphal, L. Dobrzycki, R. Boese and S. Harder, *Chem. Commun.*, 2010, **46**, 7757–7759; (*c*) M. Carrasco, R. Peloso, A. Rodríguez, E. Álvarez, C. Maya and E. Carmona, *Chem. – Eur. J.*, 2010, **16**, 9754–9757; (*d*) K. Freitag, H. Banh, C. Ganesamoorthy, C. Gemel, R. W. Seidel and R. A. Fischer, *Dalton Trans.*, 2013, **42**, 10540–10544.
12 T. Bollermann, C. Gemel and R. A. Fischer, *Coord. Chem. Rev.*, 2012, **256**, 537–555.
13 M. Carrasco, R. Peloso, I. Resa, A. Rodríguez, L. Sánchez, E. Álvarez, C. Maya, R. Andreu, J. J. Calvente and A. Galindo, *Inorg. Chem.*, 2011, **50**, 6361–6371.
14 (*a*) A. Lühl, L. Hartenstein, S. Blechert and P. W. Roesky, *Organometallics*, 2012, **31**, 7109–7116; (*b*) A. Lühl, H. P. Nayek, S. Blechert and P. W. Roesky, *Chem. Commun.*, 2011, **47**, 8280–8282.
15 (*a*) P. Mahawar, T. Rajeshkumar, T. P. Spaniol, L. Maron and J. Okuda, *Inorg. Chem.*, 2024, **63**, 8493–8501; (*b*) B. Li, K. Huse, C. Wolper and S. Schulz, *Chem. Commun.*, 2021, **57**, 13692–13695; (*c*) S. Xu, Q. Wang, T. Rajeshkumar, S. Jiang, L. Maron and X. Xu, *J. Am. Chem. Soc.*, 2024, **146**, 19590–19598; (*d*) P. Mahawar, T. Rajeshkumar, T. P. Spaniol, L. Maron and J. Okuda, *Chem. Commun.*, 2024, **60**, 11359–11362; (*e*) S. Jiang, Y. Cai, T. Rajeshkumar, I. del Rosal, L. Maron and X. Xu, *Angew. Chem., Int. Ed.*, 2023, **62**, e202307244; (*f*) B. Li, C. Wölper, K. Huse and S. Schulz, *Chem. Commun.*, 2020, **56**, 8643–8646; (*g*) T. D. Lohrey, L. Maron, R. G. Bergman and J. Arnold, *J. Am. Chem. Soc.*, 2019, **141**, 800–804; (*h*) S. Gondzik, D. Bläser, C. Wölper and S. Schulz, *J. Organomet. Chem.*, 2015, **783**, 92–95.
16 W. Yang, A. J. P. White and M. R. Crimmin, *Nat. Synth.*, 2025, **4**, 995–1000.
17 S. Gondzik, S. Schulz, D. Bläser and C. Wölper, *Chem. Commun.*, 2014, **50**, 1189–1191.
18 S. Xu, S. Jiang and X. Xu, *Polyhedron*, 2023, **242**, 116525.
19 (*a*) M. J. C. Dawkins, E. Middleton, C. E. Kefalidis, D. Dange, M. M. Juckel, L. Maron and C. Jones, *Chem. Commun.*, 2016, **52**, 10490–10492; (*b*) A.-K. Wiegand, A. Rit and J. Okuda, *Coord. Chem. Rev.*, 2016, **314**, 71–82; (*c*) M. M. D. Roy, A. A. Omaña, A. S. S. Wilson, M. S. Hill, S. Aldridge and E. Rivard, *Chem. Rev.*, 2021, **121**, 12784–12965; (*d*) A. Kreider-Mueller, P. J. Quinlivan, M. Rauch,

J. S. Owen and G. Parkin, *Chem. Commun.*, 2016, **52**, 2358–2361; (*e*) J. G. Melnick, A. Docrat and G. Parkin, *Chem. Commun.*, 2004, 2870–2871; (*f*) A. Pöllnitz, C. Silvestru, J.-F. Carpentier and A. Silvestru, *Dalton Trans.*, 2012, **41**, 5060–5070.

20 (*a*) P. Granger, S. Chapelle, W. R. McWhinnie and A. Al-Rubaie, *J. Organomet. Chem.*, 1981, **220**, 149–158; (*b*) G. Balzer, H. Duddeck, U. Fleischer and F. Röhr, *Fresenius J. Anal. Chem.*, 1997, **357**, 473–476.

21 Y.-W. Jun, C.-S. Choi and J. Cheon, *Chem. Commun.*, 2001, 101–102.

22 (*a*) A. K. Verma, T. B. Rauchfuss and S. R. Wilson, *Inorg. Chem.*, 1995, **34**, 3072–3078; (*b*) S. Dev, E. Ramli, T. B. Rauchfuss and C. L. Stern, *J. Am. Chem. Soc.*, 1990, **112**, 6385–6386; (*c*) M. Ballesteros Ii and E. Y. Tsui, *Dalton Trans.*, 2020, **49**, 16305–16311; (*d*) G. K. Kolluru, R. E. Shackelford, X. Shen, P. Dominic and C. G. Kevil, *Nat. Rev. Cardiol.*, 2023, **20**, 109–125; (*e*) K. Hossain, S. Atta, A. B. Chakraborty, S. Karmakar and A. Majumdar, *Chem. Commun.*, 2024, **60**, 4979–4998.

23 (*a*) C. Kimblin, W. E. Allen and G. Parkin, *J. Chem. Soc., Chem. Commun.*, 1995, 1813–1815; (*b*) E. Jaime, A. N. Kneifel, M. Westerhausen and J. Weston, *J. Organomet. Chem.*, 2008, **693**, 1027–1037; (*c*) S. Schulz, J. Spielmann, D. Bläser and C. Wölper, *Chem. Commun.*, 2011, **47**, 2676–2678; (*d*) D. Prochowicz, K. Sokołowski and J. Lewiński, *Coord. Chem. Rev.*, 2014, **270–271**, 112–126.

24 (*a*) CCDC 2482300: Experimental Crystal Structure Determination, 2025, DOI: 10.5517/ccdc.csd.cc2pb169; (*b*) CCDC 2482301: Experimental Crystal Structure Determination, 2025, DOI: 10.5517/ccdc.csd.cc2pb17b; (*c*) CCDC 2482302: Experimental Crystal Structure Determination, 2025, DOI: 10.5517/ccdc.csd.cc2pb18c; (*d*) CCDC 2482303: Experimental Crystal Structure Determination, 2025, DOI: 10.5517/ccdc.csd.cc2pb19d; (*e*) CCDC 2482304: Experimental Crystal Structure Determination, 2025, DOI: 10.5517/ccdc.csd.cc2pb1bf; (*f*) CCDC 2482305: Experimental Crystal Structure Determination, 2025, DOI: 10.5517/ccdc.csd.cc2pb1cg; (*g*) CCDC 2482306: Experimental Crystal Structure Determination, 2025, DOI: 10.5517/ccdc.csd.cc2pb1dh; (*h*) CCDC 2496490: Experimental Crystal Structure Determination, 2025, DOI: 10.5517/ccdc.csd.cc2pssy7; (*i*) CCDC 2496491: Experimental Crystal Structure Determination, 2025, DOI: 10.5517/ccdc.csd.cc2pssz8.